Combinatorial Screening of Inkjet Printed Ternary Blends for Organic Photovoltaics: Absorption Behavior and Morphology

Anke Teichler,[†,‡,§] Stefan Hölzer,[†,‡] Jürgen Nowotny,[†,‡] Florian Kretschmer,[†,‡] Cornelia Bader,[†,‡] Jolke Perelaer,[†,‡,§] Martin D. Hager,[†,‡,§] Stephanie Hoeppener,[†,‡] and Ulrich S. Schubert*[,†,‡,§]

[†]Laboratory of Organic and Macromolecular Chemistry (IOMC), Friedrich Schiller University Jena, Humboldtstraße 10, 07743 Jena, Germany

[‡]Jena Center for Soft Matter (JCSM), Philosophenweg 7, 07743 Jena, Germany

[§]Dutch Polymer Institute (DPI), P.O. Box 513, 5600 MB Eindhoven, The Netherlands

ABSTRACT: Inkjet printing was used for the preparation of ternary polymer/polymer/fullerene layers for organic solar cell application, as part of a combinatorial setup for the preparation and characterization of thin-film libraries. Poly(phenylene-ethynylene)-*alt*-poly(phenylene-vinyl-ene) (PPE-*alt*-PPV) and poly(diketopyrrolopyrrole-*alt*-fluorene) (P(DPP-*alt*-F)) were systematically blended with poly(3-octylthiophene) (P3OT) and investigated by UV−vis spectroscopy to improve the photon harvesting by extending the absorption range. The blends with the broadest absorption range (20 and 40 wt % of PPE-*alt*-PPV and P(DPP-*alt*-F), respectively) were mixed with mono(1-[3-(methoxycarbonyl)propyl]-1-phenyl)-[6,6]C$_{61}$ (PCBM). The blend with the low band gap polymer P(DPP-*alt*-F) revealed the most extended absorption, which ranges over the whole visible spectrum (350 to 750 nm). The mixing with PCBM (ratio 1/3) led to an optimal emission quenching and revealed a smooth film formation. In this contribution, we show that the combinatorial screening using inkjet printing represents an effective, time- and material-saving workflow for the investigation of polymer blend libraries, which is of high interest for the development of new materials for active layers in organic photovoltaics.

KEYWORDS: *combinatorial screening, inkjet printing, ternary blends, absorption, morphology*
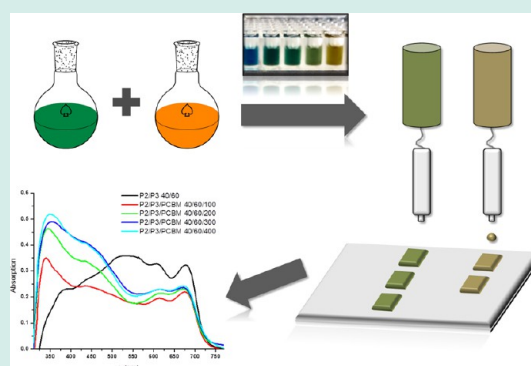
INTRODUCTION

The development of smaller, more flexible and cheaper optoelectronic devices, for example, organic light emitting diodes (OLEDs)[1] and organic photovoltaics (OPVs),[2] benefits from the tunable characteristics of conjugated polymers, in particular variable optical properties. Conjugated polymer structures in the field of OPVs include poly(phenylene-vinylene) (PPV),[3,4] poly(phenylene-ethynylene)-*alt*-poly-(phenylene-vinylene) (PPE-*alt*-PPV),[5,6] poly(thiophene) (PT),[7,8] poly(fluorene) (PF),[9,10] and poly-(diketopyrrolopyrrole) (PDPP).[11,12]

Thereby, a low polymer band gap[2] as well as a broad absorption range are required to improve quantum efficiencies of the final organic solar cell devices.[13] For instance, low band gap donor−acceptor copolymers were found to reveal improved photon harvesting properties.[14,15] In the past years, DPP moieties have gained an increased interest as a building unit for polymers used for organic solar cells because of their strong absorption in the visible region and their electron-withdrawing behavior.[16] For this reason, DPP represents a suitable building moiety for donor−acceptor polymers. Fluorene (F) moieties are rigid and planar building units that in contrast to DPP, act as an electron-donating unit.[17] As a

result, P(DPP-*alt*-F) is a donor−acceptor copolymer, which represents a low-band gap polymer.[18] Although fine-tuning of the optical properties can be enabled by attaching side chains to the polymer backbone, the polymer shows absorption only in a specific wavelength-range.

A straightforward approach to increase the absorption range is blending of two polymers with different absorption characteristics. Improved performances of organic solar cell devices have been reported in literature by using a ternary mixture of polymer/polymer/fullerene[19,20] or polymer/small molecule/fullerene.[21] Thereby, the fullerene derivatives act as electron acceptor in the active layer.

For the preparation of the active layer of an organic solar cell, inkjet printing as well as spin-coating can be used as solution deposition method.[22,23] In contrast to spin-coating, where more than 90% of the material is wasted, inkjet printing represents a highly material-efficient deposition method that requires only small amounts of functional materials and produces a minimal
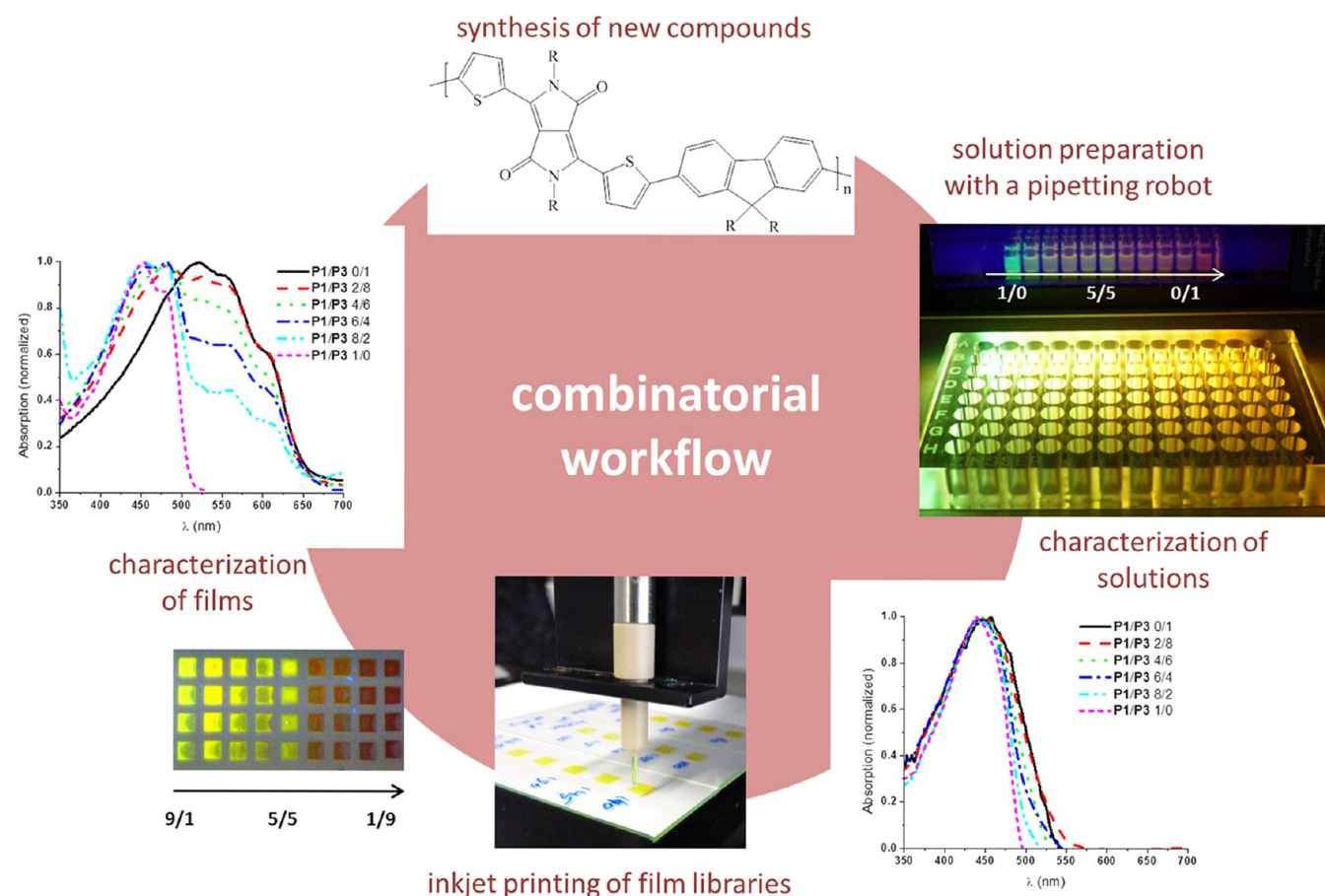
Figure 1. Experimental workflow for the combinatorial screening of binary polymer/polymer and ternary polymer/polymer/fullerene blends for the use in organic solar cells.

amount of waste, since the material is placed on-demand and where required.[24,25]

Many processing parameters influence the fabrication of the active layer and, as a consequence, the final device properties. Ink formulations, like the solvent, the concentration, and the polymer/fullerene ratio, as well as the process parameters, including film thickness, temperature, and, obviously, the processing technique itself, have a significant influence on the properties of the active layer. Furthermore, with the addition of more components to the mixture the number of combinations is exponentially increasing.

Therefore, a combinatorial screening approach is necessary to elucidate important structure−property relationships as well as to identify the most promising blends and blend ratios for the use as active bulk heterojunction solar cell layers. To reveal correlations between printing conditions and solar cell activities the investigation of the performance of the inkjet printed active layers in solar cells is the scope of future publications.

Inkjet printing is a precise and noncontact patterning technique, which can be used as a combinatorial screening tool to discover quantitative structure−property relationships, as described recently for the optimization of donor/acceptor materials for solar cells.[26,27] By using inkjet printing, synergies between ink properties and film characteristics can be found,[28] which significantly accelerates research and, subsequently, leads to a fast and simple handling of promising compounds for OPVs. Because of the continuous development of new polymers, many blend combinations might be promising as active layers. By using the presented workflow high perform-

ance materials and mixtures can be identified in a time- and material-efficient procedure.

In this contribution, we report the screening of two polymer/polymer blends, using a combinatorial experimental setup. To optimize the absorption of the active layer materials, two blend systems from poly(3-octylthiophene) (P3OT) with (i) PPE-*alt*-PPV and (ii) P(DPP-*alt*-F) were investigated according to their film formation and optical behavior.

■ RESULTS AND DISCUSSION

Combinatorial screening. The experimental setup for the combinatorial screening of various binary polymer/polymer and ternary polymer/polymer/fullerene mixtures is depicted in Figure 1. The following combinatorial workflow was used:

(i) The mixtures with the desired compound ratios, solvent system, and concentration were prepared in a quartz 96-well microtiter plate. For each polymer a solvent mixture of chlorobenzene/*ortho*-dichlorobenzene (CB/*o*-DCB) in a ratio of 90/10 was used.

(ii) The filled microtiter plate was used for UV−vis absorption and emission measurements of the blend solutions with a UV−vis plate reader.

(iii) Individual wells of the plate were used as small solution reservoirs for the inkjet printing process.

(iv) Thin-film libraries were printed in a microtiter plate pattern according to the positions to the wells of a 96-well plate to screen the optical properties of the films using a high-throughput UV−vis plate reader.

Single Polymers. At first, the individual polymers poly-(phenylene-ethynylene)-*alt*-poly(phenylene-vinylene) (PPE-*alt*-PPV) **P1** (Figure 2a), poly(diketopyrrolopyrrole-*alt*-fluo-

Figure 2. Schematic representation of the chemical structure of the investigated polymers. (**a**) Poly(phenylene-ethynylene)-*alt*-poly-(phenylene-vinylene) **P1** (R₁ = octyl, R₂ = octadecyl), (**b**) poly-(diketopyrrolopyrrole-*alt*-fluorene) **P2** (R = ethylhexyl on DPP, octyl on F) and (**c**) poly(3-octylthiophene) **P3** (R = octyl).

rene) P(DPP-*alt*-F) **P2** (Figure 2b), and poly(3-octylthio-phene) (P3OT) **P3** (Figure 2c) were investigated concerning their printability, film formation, and absorption behavior in solution and film. The results are summarized in Table 1. The surface roughness R_a of **P1**, **P2**, and **P3**, as estimated by optical interferometry, was found to be 8, 15, and 30 nm, respectively (Table 1). Thus, the film formation via inkjet printing seems to be better for the polymers **P2** and **P3** under the given processing conditions.
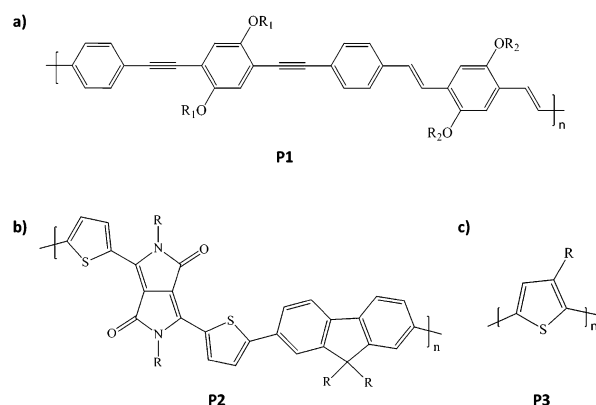
To investigate the polymers as potential candidates for the use in ternary mixtures, the absorption of the single polymers in solution and as film needs to be measured. **P1** reveals in solution an absorption maximum at 443 nm (Figure 3a), whereas two absorption peaks are observed in the inkjet printed film at 451 and 480 nm (Figure 3c). A red-shift of the absorption peak in the solid state occurs because of an improved planarization of the polymer backbone.[29] According to literature, the revealed band-splitting in the film absorption spectra is correlated to the formation of aggregates.[30]

The absorption spectrum of the **P2** solution shows four peaks, which can be assigned to moieties of PDPP (417 nm, 609 nm, 661 nm) and PF (370 nm, Figure 3b). The absorption of **P2** of a printed film reveals only a small red-shift in comparison to the solution (Figure 3d). In contrast, polymer **P3** shows a more significant bathochromic shift between the solution (454 nm, Figure 3a) and the inkjet printed film ((522 nm, Figure 3c). Thereby, the three absorption peaks of

the inkjet printed film can be assigned to the $\pi-\pi^*$ transition (522 nm) and interchain interactions (550 nm, 610 nm). This behavior can be explained by an improved planarization and aggregation of the polymer in the solid state.[29]

The optical band gap of all three polymers was determined from the UV−vis spectra of the polymers in solution (Table 1).[31] The different optical properties of **P1**, **P2**, and **P3** can be explained by their chemical structures taking structural criteria for the design of conjugated polymers with reduced bandgaps into consideration.[2] **P1** has a relative high optical band gap of 2.4 eV, which is not favorable for their use in OPV as a single photon harvesting species. The high bandgap originates from a single bond rotation and therefore, from the hindered formation of the quinoid structure and delocalization of π-electrons. **P3** has a lower bandgap of 1.9 eV because of the high density of bulky side-chains, which cause a steric hindrance of the single bond rotation. Therefore, **P3** has a higher planarity of the aromatic backbone, which results in a higher degree of delocalization of π-electrons. Furthermore, the absorption spectrum of **P3** in the solid state is characterized by PT crystals that lead to a more ordered phase of the polymer and, hence, to a lower bandgap.[18] The copolymer of PDPP and PF, **P2**, reveals a band gap of 1.7 eV, which is classified as being a low bandgap polymer and which is favorable for solar cell applications.[11] Copolymer **P2** has a very rigid structure that does not undergo further planarization in the solid state and, as a consequence, no strong red-shift of the absorption in the solid state compared to the solution is observed.

Polymer/Polymer Blends. Since all individual polymers **P1**, **P2**, and **P3** show different absorption spectra in the solid state, a combination of the polymers is promising to improve the overall yield of photon harvesting.

The first investigated polymer/polymer blend consists of **P1**/**P3**. The polymers were mixed in different ratios ranging from 8/2 to 2/8 by weight. The absorption spectra of the blends in solution (Figure 3a) showed a single absorption peak at 439 nm for the ratio 8/2, which is compared to **P1** 4 nm blue-shifted. With increasing **P3**-content the maximum peak shifts to 445 nm for the ratio 2/8 and the absorption spectra become broader.

The spectra of the inkjet printed films of the blends **P1**/**P3** (Figure 3c) show a broad absorption from 350 to 650 nm; the observed absorption features can be assigned to **P1** (452 nm, 480 nm) and **P3** (557 nm, 610 nm, Table 1). Thereby, the intensity of the two absorption peaks at 557 and 610 nm increases systematically with the **P3**-content. However, even with a high **P3**-content in the blend, the **P1** absorption peaks show high intensities because of a high absorption coefficient of the **P1** material.[32] This implies that only a small addition of **P1** is required to increase the total absorption range of the polymer films significantly. Upon decreasing **P1**-content in the blend,

Table 1. Optical Properties in Solution and as Inkjet Printed Film As Well As Film Formation Characteristics of the Pristine Polymers P1, P2, and P3 and the Binary Blends P1/P3 2/8 and P2/P3 4/6

	solution		inkjet printed film			
	$\lambda_{max,\ abs}$ [nm]	E_g^{opt} [eV]	$\lambda_{max,\ abs}$ [nm]	film thickness [nm]	surface roughness R_a [nm]	dot spacing [μm]
P1	443	2.43	451	160	30	120
P2	661	1.70	660	190	8	100
P3	454	1.89	522	150	15	160
P1/P3 (2/8)	445		482	140	30	100
P2/P3 (4/6)	660		666	170	20	110
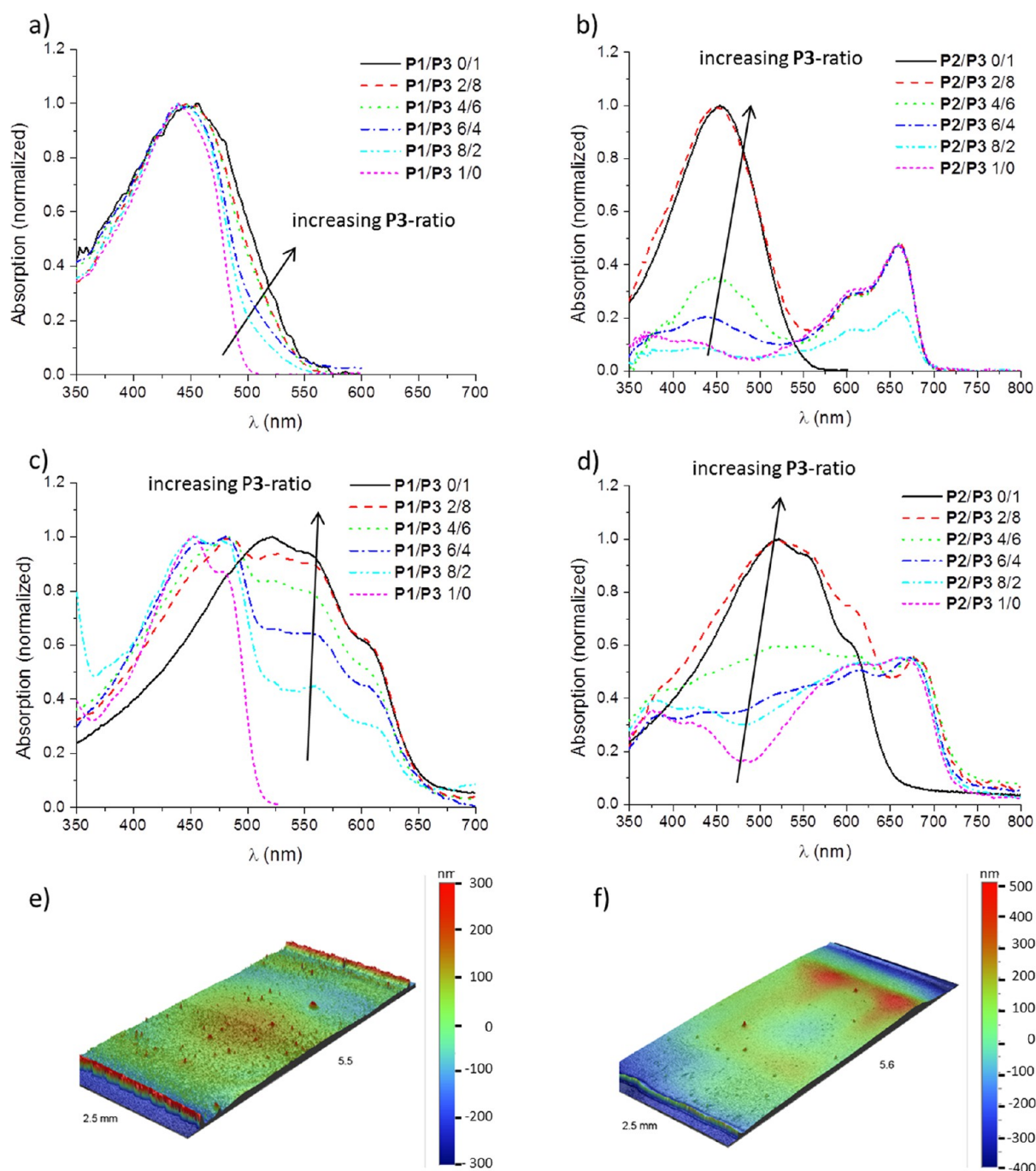
Figure 3. Absorption spectra of **P1**, **P3**, and **P1/P3** blends (a) and **P2**, **P3**, and **P2/P3** blends (b) in solution and inkjet printed films (c, d). Optical profiler images of the inkjet printed blend films **P1/P3** 2/8 (e) and **P2/P3** 4/6 (f).

the absorption peak of **P1** (452 nm) shifts to 462 nm. Further decreasing of the **P1**-content leads to lower intensities. It can be assumed that the polymer **P1** shows with increased **P3**-content a preferred formation of aggregates (as observed by the absorption at 480 nm) when inkjet printed from a **P1/P3** mixture.[30] From Figure 3c it can be concluded that the blend ratio **P1/P3** 2/8 shows the best absorption performance, since the absorption range is the broadest when compared to the other ratios.

Figure 3e shows an optical profilometer image of the blend ratio **P1/P3** 2/8. Although inkjet printing of the films was performed directly after mixing the polymers and the mixtures are continuously stirred during printing, rough films with a

surface roughness R_a of 30 to 40 nm were formed. In contrast, a smooth surface with R_a of 15 nm was obtained when printing the single polymer **P3** using the same solvent. The binary blends containing **P1** and **P3** reveal a similar roughness as the single polymer **P1** (Table 1).

In summary, blending **P3** with a small amount of **P1** copolymer leads to an increased absorption range in the region from 350 to 630 nm. However, to improve the solar emission match, an absorption at higher wavelengths is required.[13]

Figure 3b shows the absorption spectra for the mixtures of **P2** and **P3** in solution. The peak at around 450 nm is assigned to **P3** and the peaks at 376 nm, 430 nm, 608 nm, and 660 nm to **P2**. In the region between 430 and 450 nm, an overlay of
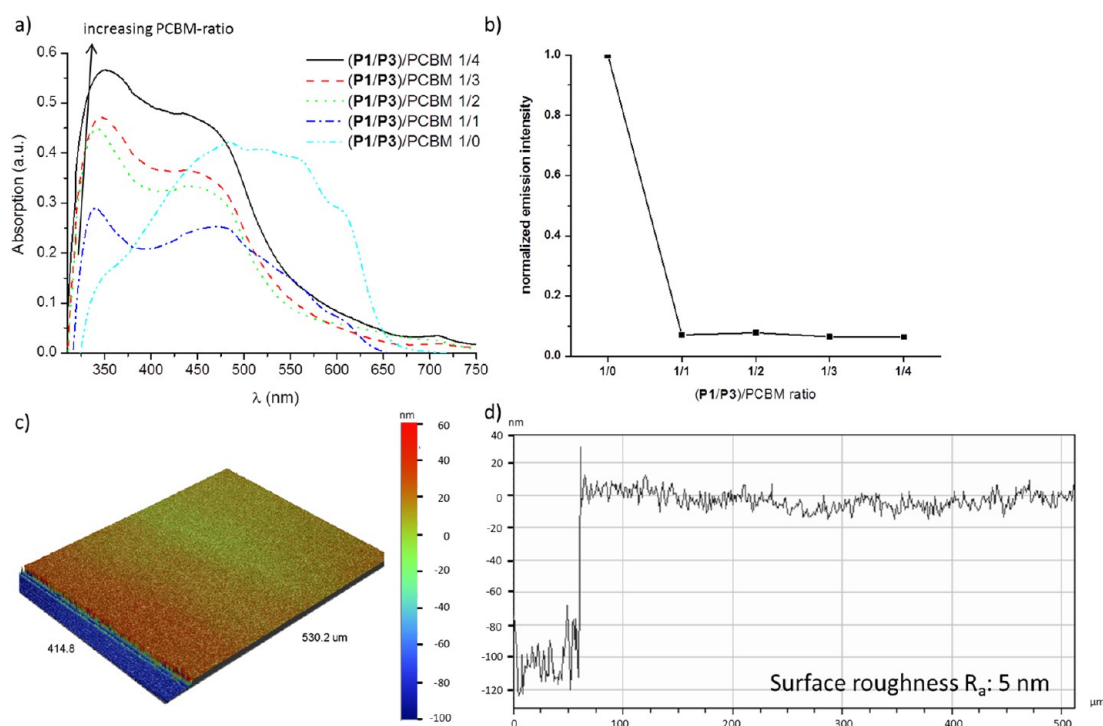
Figure 4. Absorption spectra (a) and normalized photoluminescence spectra (b) of inkjet printed films of **P1**/**P3** 2/8 in the mixture with PCBM with varied polymer/PCBM ratios. Optical profiler image (c) and corresponding cross-section (d) of an inkjet printed film of the polymer/PCBM ratio 1/1.

absorption from both polymers is observed. After printing, the UV−vis spectra show a significant broadening in the region of 650 to 750 nm, by adding a small fraction of **P2**, leading to an overall absorption range between 350 and 750 nm (Figure 3d). The absorption peaks of the printed samples are in comparison to the absorption in solution more structured as well as red-shifted; **P3** (520 nm, 550 nm, 610 nm) and **P2** (383 nm, 435 nm, 610 nm, 673 nm). From the absorption spectra in Figure 3d it was concluded that the blend ratio **P2**/**P3** 4/6 shows the broadest and most intense absorption of the investigated blends. Hence, this ratio was used for further investigations. In Figure 3f an optical profilometer image of an inkjet printed film of the blend ratio 4/6 is depicted. The image represents a 170 nm thick film with a surface roughness R_a of 20 nm (Table 1).

It is worth noting that the specific P3OT interchain interactions in the solid state (**P3**, 550 nm, 610 nm) is still observed when mixed with **P1** or **P2**, even at low **P3** contents. Thus, it can be assumed that the addition of **P1** or **P2** does not suppress the formation of highly ordered thiophene crystals.

Polymer/Polymer/Fullerene Blends. *Optical Properties.* As described in the previous sections the blend mixtures **P1**/**P3** 2/8 and **P2**/**P3** 4/6 were chosen from the combinatorial study of the binary blends for further investigations. Ternary blends were prepared from these mixtures by adding mono(1-[3-(methoxycarbonyl)propyl]-1-phenyl)-[6,6]C_{61} (PCBM) as electron-accepting unit, which is commonly used in active layers of organic solar cells. The chosen polymer blend/PCBM ratios of 1/1, 1/2, 1/3, and 1/4 were inkjet printed and investigated according their film formation behavior and optical properties.

Figure 4a shows the absorption spectra of inkjet printed films of the ternary blends that consist of **P1**/**P3** 2/8 and PCBM in the prescribed ratios. The absorption peak at 320 nm originates

from the fullerene derivative and increases in intensity with the PCBM content in the blend. The wavelength, at which the polymer **P3** absorbs in the ternary blend, differs from the binary polymer/polymer mixture. Whereas in the spectrum of the polymer/PCBM ratio 1/1 the absorption bands of **P3** (520 nm, 550 nm, 610 nm) are still visible, this band structure is not observed at higher PCBM contents. For the films with a higher fullerene content only a blue-shifted main absorption peak of the $\pi-\pi^*$ transition is present. This is an indication for reduced interchain interactions of **P3** in the presence of PCBM in the blend. The polymer emission is quenched by a factor of 10 when PCBM was added in a ratio of polymer/PCBM 1/1, as can be seen in Figure 4b. Increasing the amount of PCBM did not lead to a further decrease of the polymer emission. The significant quenching is an indication for a good mixing of the components in the ternary blends, which lead to an efficient charge transfer from the electron-donator to the electron-acceptor.

The absorption spectra of the polymer blend **P2**/**P3** 4/6 in a mixture with different amounts of PCBM are shown in Figure 5a. Similar to the (**P1**/**P3**)/PCBM blend, the intensity of the absorption peak at 320 nm is increasing with higher PCBM contents. Figure 5b shows the emission measurements of the (**P2**/**P3**)/PCBM blends. A high quenching of the emission was observed for all investigated (**P2**/**P3**)/PCBM blends. The maximum quenching was found for a ratio of ((4/6)/30) (Figure 5b), indicating an appropriate charge transfer in the blend. A quick indication of effective mixing and charge separation could be obtained by measuring the photo-luminescence quenching of the ternary blends. Combinatorial screening of different blend compositions yields the most promising mixtures, based on the optical and film formation behavior, being (**P1**/**P3**)/PCBM ((2/8)/10) and (**P2**/**P3**)/PCBM ((4/6)/30), respectively.
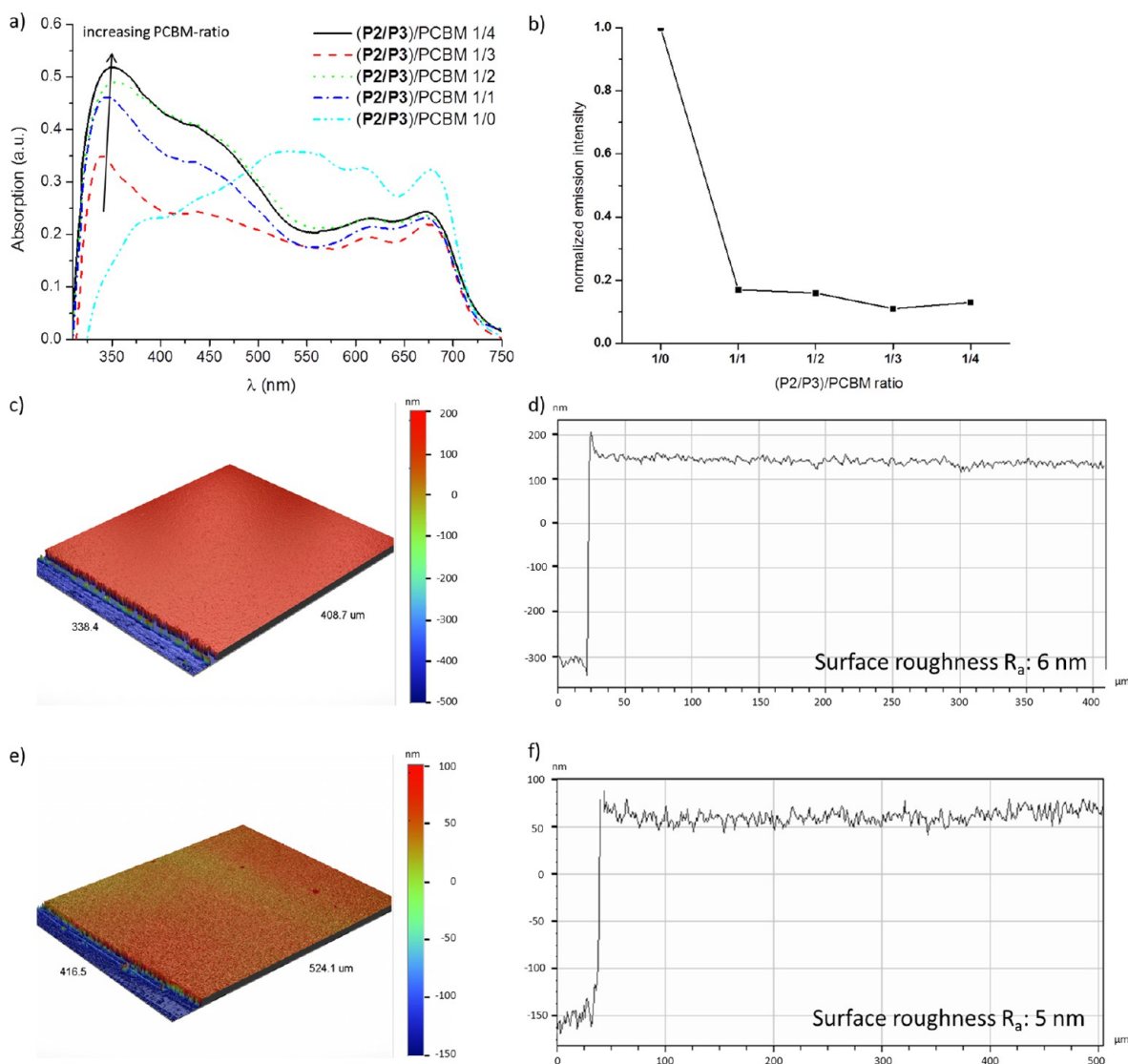
Figure 5. Absorption spectra (a) and normalized photoluminescence spectra at maximum (b) of inkjet printed films of **P2/P3** 4/6 in the mixture with PCBM with varied polymer/PCBM ratios. Optical profiler images (c, e) and corresponding cross sections (d, f) of inkjet printed films of the polymer/PCBM ratio 1/3 with a concentration of 0.8 wt % (c, d) and 0.5 wt % (e, f).

Morphological Characterization. The optical profilometer image of the inkjet printed film of the blend (**P1/P3**)/PCBM (2/8)/10 is depicted in Figure 4c, which shows a smooth film with a thickness of approximately 100 nm and a surface roughness R_a of 5 nm (Figure 4d). In Figure 5c an optical profiler image of an inkjet printed film of the blend (**P2/P3**)/ PCBM (4/6)/30 is depicted, which demonstrates a smooth film formation (R_a = 6 nm) with a thickness of approximately 450 nm (Figure 5d). To reveal the required optimal thickness for an active layer of solar cells, which is between 100 and 200 nm,[13] the concentration was reduced to 0.5 wt %, leading to a film thickness of approximately 200 nm with a low roughness (R_a = 5 nm), as depicted in Figure 5e,f.

The active layer morphology affects the charge transport through the active layer and is crucial for an evaluation of applicable polymer/fullerene blends or active layer preparation conditions for OPVs.[33] Therefore, atomic force microscopy (AFM) measurements were performed on selected blends, although the required time for these measurements is far too long for a combinatorial screening method.

AFM images of the P1/PCBM 1/1 blend reveals a rough film with R_a of 17 nm (Figure 6a), which is also reflected in the results from the interferometric profiler. Inkjet printing of the PPE-*alt*-PPV polymer in the mixture with PCBM reveals an unfavorable morphology by the formation of PCBM clusters and a strong phase separation of the individual compounds. This observation is in good agreement with literature.[6]

For the binary polymer/fullerene blends P2/PCBM 1/3 (Figure 6b) and P3/PCBM 1/1 (Figure 6c) smooth film surfaces with R_a of 1 nm are obtained. The inkjet printed film of P2/PCBM reveals different phases in the range of 10 nm, which is reported to be suitable for active layer morphologies.[34]

P3/PCBM films prepared by inkjet printing from CB/*o*-DCB revealed fibrillar domains of P3OT that represent a highly ordered self-organization of the chains (Figure 6f). Note that the differences between the domain spacing in Figure 6f (being approximately 10 nm in the image) and the real distances between the thiophene crystals (of approximately 1 nm)[35] are screened by the convolution with dimensions of the AFM tip. The morphology observed for the as-printed film is comparable to the spin-coated films after annealing or additive addition.[34,36]
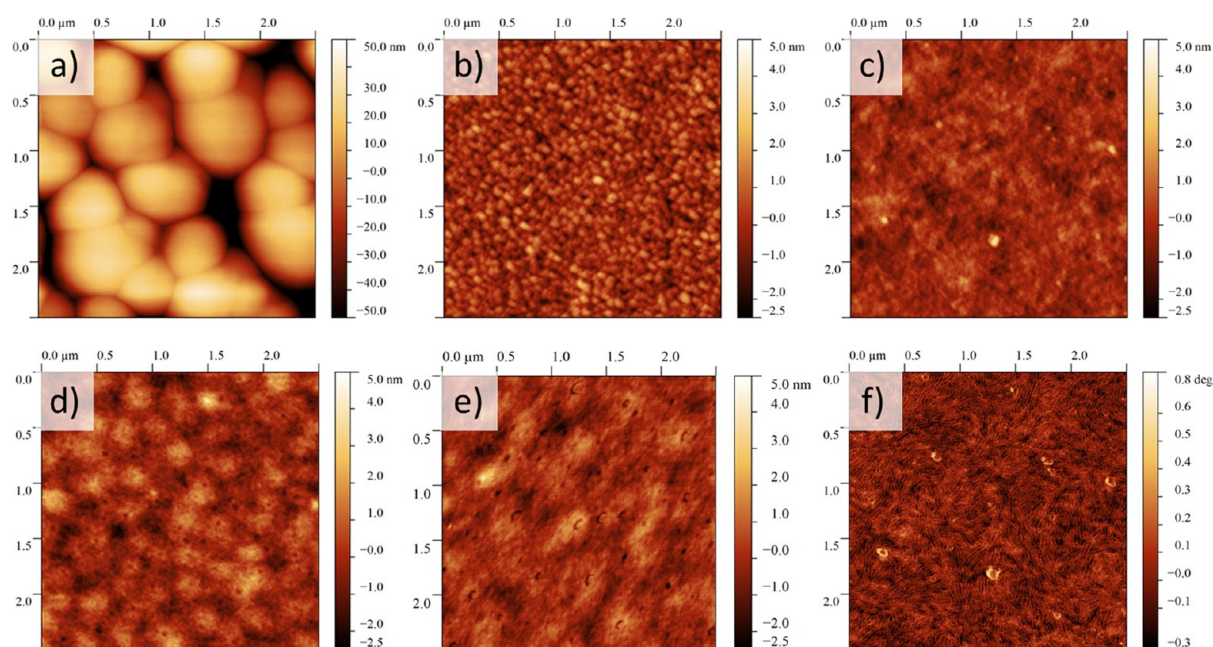
Figure 6. Atomic force microscopy height images of inkjet printed films of **P1**/PCBM 1/1 (a), **P2**/PCBM 1/3 (b), **P3**/PCBM 1/1 (c), (**P1**/**P3**)/PCBM (2/8)/10 (d), and (**P2**/**P3**)/PCBM 4/6/30 (e). Phase image of inkjet printed **P3**/PCBM 1/1 blend (f).

In the presence of PCBM, polythiophenes typically lose their chain alignment. As a result, postprocessing annealing methods, like thermal or solvent annealing, were developed to reorganize the polythiophene chains into the preferred fibrillar structure, which result in improved charge transport properties. As shown here, P3OT reveals self-organized domains in the blend with PCBM already in the as-inkjet printed films (Figure 6f). The reasons for the differences in film formation characteristics are explained by the use of the different film preparation techniques as well as processing solvents. When using conditions that cause a slow film drying, for example, by inkjet printing or by using the high boiling solvent chlorobenzene, the polythiophene chains may form highly ordered structures already during drying of the film. In contrast, when the drying proceeds too fast, for example, by using spin-coating or the low boiling solvent chloroform, the formation of the thermodynamically preferred crystalline polythiophene phases cannot take place.

AFM measurements of the ternary blends (**P1**/**P3**)/PCBM (2/8)/10 (Figure 6d) and (**P2**/**P3**)/PCBM (4/6)/30 (Figure 6e) revealed smooth (surface roughness $R_a = 1$ nm) and well mixed layer morphologies. The typical main chain crystals of the P3OT, which are observed in the binary **P3**/PCBM blend, were not observed in the ternary blend films. This is in agreement with the findings of the absorption spectra of the (**P2**/**P3**)/PCBM blend, where only weak signals were found, which correspond to the P3OT interchain interactions. The band structure of **P3** was observed in the absorption spectra of both binary blends, **P1**/**P3** 2/8 and **P2**/**P3** 4/6. Hence interchain interactions of **P3** should also occur in polymer/**P3** blends. As a result, the interruption of the self-organization of P3OT is only observed in the ternary blend film. Although improved absorption characteristics of the ternary blend films are observed, morphological investigations reveal an unpreferred P3OT morphology in comparison to the binary P3OT/PCBM mixture. To answer the question whether the successful mixing of two polymers with PCBM in a ternary blend reveals an enhanced photon harvesting, solar cell characteristics need to be measured, which will be executed in the future.

Since not only optical film characteristics but also morphological properties are important for an evaluation of promising donor/acceptor blends for solar cells, the combinatorial screening workflow presented here can only reduce the amount of samples to be tested, but cannot provide a selection of one best donor/acceptor combination. Since morphological investigations represent a serious bottleneck for a fast and efficient screening procedure, the combinatorial screening workflow, which allows to identify promising formulations and reveals a reduction of the amount of samples, is of high importance.[37]

■ CONCLUSIONS

We have demonstrated that the mixing of conjugated polymers represents a straightforward strategy for improving the absorption of the active layers for organic solar cells. An experimental setup for a combinatorial screening was presented here to investigate the absorption behavior of polymer/polymer blends in solution and films. The used polymers include poly(phenylene-ethynylene)-*alt*-poly(phenylene-vinylene) (PPE-*alt*-PPV), poly(diketopyrrolopyrrole-*alt*-fluorene) (P-(DPP-*alt*-F)), and poly(3-octylthiophene) (P3OT). An optimum absorption spectrum was found when mixing the compounds P(DPP-*alt*-F) and P3OT in a ratio of 4/6, while a quenching optimum was revealed when using a polymer/PCBM ratio of 1/3.

This ternary blend was found to cover a large absorption spectrum from 350 to 750 nm. Inkjet printing enabled a homogeneous film formation as well as a successful combinatorial screening of thin film properties of various compounds and blends for possible solar cell applications that lead to important structure−property-relationships. The next steps include the investigations of the inkjet printed active layers for their solar cell activity and the measurements of the resulting power conversion efficiencies.

■ EXPERIMENTAL PROCEDURES

Materials. The polymers poly(phenylene-ethynylene)-*alt*-poly(phenylene-vinylene) (PPE-*alt*-PPV) **P1** (M_n = 10,200 g·mol^{-1}, M_w = 39,400 g·mol^{-1}, PDI = 3.86) and poly-(diketopyrrolopyrrole-*alt*-fluorene) (P(DPP-*alt*-F)) **P2** (M_n = 26,000 g·mol^{-1}, M_w = 56,000 g·mol^{-1}, PDI = 2.15) were synthesized as described elsewhere.[11,32] Poly(3-octylthiophene) (P3OT) **P3** (M_n = 34,500 g·mol^{-1}), mono(1-[3-(methoxycarbonyl)propyl]-1-phenyl)-[6,6]C$_{61}$ (PCBM), the used solvents chlorobenzene (CB) and *ortho*-dichlorobenzene (*o*-DCB) were purchased from Sigma-Aldrich (Steinheim, Germany) and were used without further purification. The polymers were dissolved in the required ratios in a solvent mixture of CB and *o*-DCB with a concentration of 0.8 wt % and 0.5 wt %, respectively, which is known to show a stable droplet formation and enables a homogeneous thin-film formation of such polymers.[26,28] For the ternary blends, the fullerene derivative was added to the polymer mixtures by using a constant polymer concentration. The solutions were filtered before printing (pore size 1 μm) to prevent nozzle clogging. Glass slides (3 × 1 in.) were used as substrates and cleaned before printing by first rinsing with *iso*-propanol and subsequent drying with an air flow.

Instrumentation. UV−vis absorption and emission measurements of the blend solutions and films were carried out with a FLASHScan 530 (Analytik Jena, Jena, Germany) UV−vis plate reader. Inkjet printing was carried out with an Autodrop system from microdrop Technologies (Norderstedt, Germany). The printer was equipped with a piezo-based micropipette printhead with an inner diameter of 70 μm. A voltage of 70 V and a pulse length of 35 μs revealed a stable droplet formation for all inks in the solvent CB/*o*-DCB. The printing speed was set to 20 mm·s^{-1} for all experiments.

Surface topography and film thicknesses were measured with an optical interferometric profiler Wyko NT9100 (Veeco, Mannheim, Germany). Atomic force microscopy (AFM) measurements were performed in tapping mode with a NTegra Aura (NT-MDT, Moscow, Russia) on selected polymer/polymer/fullerene blends.

■ AUTHOR INFORMATION

Corresponding Author
*E-mail: ulrich.schubert@uni-jena.de.

Notes
The authors declare no competing financial interest.

■ ACKNOWLEDGMENTS

■ REFERENCES

(1) Grimsdale, A. C.; Chan, K. L.; Martin, R. E.; Jokisz, P. G.; Holmes, A. B. Synthesis of light-emitting conjugated polymers for applications in electroluminescent devices. *Chem. Rev.* **2009**, *109*, 897−1091.

(2) Winder, C.; Sariciftci, N. S. Low bandgap polymers for photon harvesting in bulk heterojunction solar cells. *J. Mater. Chem.* **2004**, *14*, 1077−1086.

(3) Shaheen, S. E.; Brabec, C. J.; Sariciftci, N. S.; Padinger, F.; Fromherz, T.; Hummelen, J. C. 2.5% efficient organic plastic solar cells. *Appl. Phys. Lett.* **2001**, *78*, 841−843.

(4) van Duren, J. K. J.; Yang, X. N.; Loos, J.; Bulle-Lieuwma, C. W. T.; Sieval, A. B.; Hummelen, J. C.; Janssen, R. A. J. Relating the morphology of poly(*p*-phenylene vinylene)/methanofullerene blends to solar-cell performance. *Adv. Funct. Mater.* **2004**, *14*, 425−434.

(5) Jadhav, R.; Türk, S.; Kühnlenz, F.; Cimrova, V.; Rathgeber, S.; Egbe, D. A. M.; Hoppe, H. Anthracene-containing PPE-PPV copolymers: Effect of side-chain nature and length on photophysical and photovoltaic properties. *Phys. Status Solidi A* **2009**, *206*, 2695−2699.

(6) Hoppe, H.; Egbe, D. A. M.; Muhlbacher, D.; Sariciftci, N. S. Photovoltaic action of conjugated polymer/fullerene bulk heterojunction solar cells using novel PPE-PPV copolymers. *J. Mater. Chem.* **2004**, *14*, 3462−3467.

(7) Li, G.; Shrotriya, V.; Yao, Y.; Huang, J. S.; Yang, Y. Manipulating regioregular poly(3-hexylthiophene): [6,6]-phenyl-C-61-butyric acid methyl ester blends - route towards high efficiency polymer solar cells. *J. Mater. Chem.* **2007**, *17*, 3126−3140.

(8) Schilinsky, P.; Asawapirom, U.; Scherf, U.; Biele, M.; Brabec, C. J. Influence of the molecular weight of poly(3-hexylthiophene) on the performance of bulk heterojunction solar cells. *Chem. Mater.* **2005**, *17*, 2175−2180.

(9) Pacios, R.; Bradley, D. D. C.; Nelson, J.; Brabec, C. J. Efficient polyfluorene based solar cells. *Synth. Met.* **2003**, *137*, 1469−1470.

(10) Mammo, W.; Admassie, S.; Gadisa, A.; Zhang, F. L.; Inganäs, O.; Andersson, M. R. New low band gap alternating polyfluorene copolymer-based photovoltaic cells. *Sol. Energy Mater. Sol. Cells* **2007**, *91*, 1010−1018.

(11) Zoombelt, A. P.; Mathijssen, S. G. J.; Turbiez, M. G. R.; Wienk, M. M.; Janssen, R. A. J. Small band gap polymers based on diketopyrrolopyrrole. *J. Mater. Chem.* **2010**, *20*, 2240−2246.

(12) Sonar, P.; Ng, G. M.; Lin, T. T.; Dodabalapur, A.; Chen, Z. K. Solution processable low bandgap diketopyrrolopyrrole (DPP) based derivatives: novel acceptors for organic solar cells. *J. Mater. Chem.* **2010**, *20*, 3626−3636.

(13) Günes, S.; Neugebauer, H.; Sariciftci, N. S. Conjugated polymer-based organic solar cells. *Chem. Rev.* **2007**, *107*, 1324−1338.

(14) Janietz, S.; Krueger, H.; Schleiermacher, H. F.; Würfel, U.; Niggemann, M. Tailoring of low bandgap polymer and its performance analysis in organic solar cells. *Macromol. Chem. Phys.* **2009**, *210*, 1493−1503.

(15) Roncali, J. Molecular engineering of the band gap of π-conjugated systems: Facing technological applications. *Macromol. Rapid Commun.* **2007**, *28*, 1761−1775.

(16) Huo, L. J.; Hou, J. H.; Chen, H. Y.; Zhang, S. Q.; Jiang, Y.; Chen, T. L.; Yang, Y. Bandgap and molecular level control of the low-bandgap polymers based on 3,6-dithiophen-2-yl-2,5-dihydropyrrolo-[3,4-c]pyrrole-1,4-dione toward highly efficient polymer solar cells. *Macromolecules* **2009**, *42*, 6564−6571.

(17) Cheng, Y. J.; Yang, S. H.; Hsu, C. S. Synthesis of conjugated polymers for organic solar cell applications. *Chem. Rev.* **2009**, *109*, 5868−5923.

(18) Bundgaard, E.; Krebs, F. C. Low band gap polymers for organic photovoltaics. *Sol. Energy Mater. Sol. Cells* **2007**, *91*, 954−985.

(19) Kim, H.; Shin, M.; Kim, Y. Distinct annealing temperature in polymer:fullerene:polymer ternary blend solar cells. *J. Phys. Chem. C* **2009**, *113*, 1620−1623.

(20) Kim, Y.; Shin, M.; Kim, H.; Ha, Y.; Ha, C. S. Influence of electron-donating polymer addition on the performance of polymer solar cells. *J. Phys. D: Appl. Phys.* **2008**, *41*, 225101.

(21) Huang, J. H.; Velusamy, M.; Ho, K. C.; Lin, J. T.; Chu, C. W. A ternary cascade structure enhances the efficiency of polymer solar cells. *J. Mater. Chem.* **2010**, *20*, 2820−2825.

(22) Hoth, C. N.; Choulis, S. A.; Schilinsky, P.; Brabec, C. J. On the effect of poly(3-hexylthiophene) regioregularity on inkjet printed organic solar cells. *J. Mater. Chem.* **2009**, *19*, 5398−5404.

(23) Hoth, C. N.; Schilinsky, P.; Choulis, S. A.; Brabec, C. J. Printing highly efficient organic solar cells. *Nano Lett.* **2008**, *8*, 2806−2813.

(24) Tekin, E.; Smith, P. J.; Schubert, U. S. Inkjet printing as a deposition and patterning tool for polymers and inorganic particles. *Soft Matter* **2008**, *4*, 703−713.

(25) Singh, M.; Haverinen, H. M.; Dhagat, P.; Jabbour, G. E. Inkjet Printing-Process and Its Applications. *Adv. Mater.* **2010**, *22*, 673−685.

(26) Teichler, A.; Eckardt, R.; Hoeppener, S.; Friebe, C.; Perelaer, J.; Senes, A.; Morana, M.; Brabec, C. J.; Schubert, U. S. Combinatorial screening of polymer:fullerene blends for organic solar cells by inkjet printing. *Adv. Energy Mater.* **2011**, *1*, 105−114.

(27) Marin, V.; Holder, E.; Wienk, M. M.; Tekin, E.; Kozodaev, D.; Schubert, U. S. Inkjet printing of electron donor/acceptor blends: Towards bulk heterojunction solar cells. *Macromol. Rapid Commun.* **2005**, *26*, 319−324.

(28) Teichler, A.; Eckardt, R.; Friebe, C.; Perelaer, J.; Schubert, U. S. Film formation properties of inkjet printed poly(phenylene-ethynylene)-poly(phenylene-vinylene)s. *Thin Solid Films* **2011**, *519*, 3695−3702.

(29) Miteva, T.; Palmer, L.; Kloppenburg, L.; Neher, D.; Bunz, U. H. F. Interplay of thermochromicity and liquid crystalline behavior in poly(p-phenyleneethynylene)s: π-π interactions or planarization of the conjugated backbone? *Macromolecules* **2000**, *33*, 652−654.

(30) Tekin, E.; Wijlaars, H.; Holder, E.; Egbe, D. A. M.; Schubert, U. S. Film thickness dependency of the emission colors of PPE-PPVs in inkjet printed libraries. *J. Mater. Chem.* **2006**, *16*, 4294−4298.

(31) Hellstrom, S.; Lindgren, L. J.; Zhou, Y.; Zhang, F. L.; Inganäs, O.; Andersson, M. R. Synthesis and characterization of three small band gap conjugated polymers for solar cell applications. *Polym. Chem.* **2010**, *1*, 1272−1280.

(32) Egbe, D. A. M.; Tillmann, H.; Birckner, E.; Klemm, E. Synthesis and properties of novel well-defined alternating PPE/PPV copolymers. *Macromol. Chem. Phys.* **2001**, *202*, 2712−2726.

(33) Kästner, C.; Susarova, D. K.; Jadhav, R.; Ulbricht, C.; Egbe, D. A. M.; Rathgeber, S.; Troshin, P. A.; Hoppe, H. Morphology evaluation of a polymer-fullerene bulk heterojunction ensemble generated by the fullerene derivatization. *J. Mater. Chem.* **2012**, *22*, 15987−15997.

(34) Nguyen, L. H.; Hoppe, H.; Erb, T.; Gunes, S.; Gobsch, G.; Sariciftci, N. S. Effects of annealing on the nanomorphology and performance of poly(alkylthiophene): fullerene bulk-heterojunction solar cells. *Adv. Funct. Mater.* **2007**, *17*, 1071−1078.

(35) Beiner, M.; Huth, H. Nanophase separation and hindered glass transition in side-chain polymers. *Nat. Mater.* **2003**, *2*, 595−599.

(36) Yao, Y.; Hou, J.; Xu, Z.; Li, G.; Yang, Y. Effects of solvent mixtures on the nanoscale phase separation in polymer solar cells. *Adv. Funct. Mater.* **2008**, *18*, 1783−1789.

(37) Neffati, R.; Alexeev, A.; Saunin, S.; Brokken-Zijp, J. C. M.; Wouters, D.; Schmatloch, S.; Schubert, U. S.; Loos, J. Automated scanning probe microscopy as a new tool for combinatorial polymer research: Conductive carbon black/poly(dimethylsiloxane) composites. *Macromol. Rapid Commun.* **2003**, *24*, 113−117.